# Radiation from relativistic electrons in a magnetic wiggler

A. N. Didenko, A. V. Kozhevnikov, A. F. Medvedev, M. M. Nikitin, and V. Ya. Épp

*Research Institute of Nuclear Physics at the Tomsk Polytechnic Institute*

The spectral and polarization properties of wiggler radiation of relativistic electrons have been investigated theoretically and experimentally as a function of angle in the optical region of the spectrum for motion of the electrons in a plane magnetic wiggler installed in the ring of an electron synchrotron. The properties of the first and second harmonics of the radiation are discussed. It is shown that the polarization-angular characteristics of the first harmonic of the wiggler radiation coincide with those of instantaneous synchrotron radiation; the influence of longitudinal oscillations of the electron in the wiggler on the polarization properties of the second harmonic radiation is also shown. The appreciable influence of the angular spread of the electrons in the beam on the spectral-angular distribution of the wiggler radiation is established experimentally. The good agreement of the experimental results with the theory opens up the possibility of further use of wiggler radiation for solution of a wide range of scientific and applied problems.

PACS numbers: 29.20.Lq, 29.75. + x, 41.80.Dd

## INTRODUCTION

The radiation emitted by electrons moving in a spatially periodic magnetic field attracted attention long ago.[1-7] Interest in this phenomenon has risen substantially in recent years as the result of the possibility which has appeared of generation of wiggler radiation by means of the relativistic electron beams of synchrotrons and storage rings.[3-7] Many theoretical studies have been devoted to the general analysis of the properties of wiggler radiation,[8-12] thus permitting many important regularities of the radiation to be established, as well as a number of numerical evaluations.[10,13,14] However, experimental work carried out recently on wiggler radiation[15-17] has shown that the rather general approach which exists to the theory does not yet permit a detailed and complete description of the experimental results.

In the present work we have made several assumptions which best correspond to typical experimental conditions We discuss the motion of a particle in a magnetic field varying along the axis of motion of the electron according to a sinusoidal law. Radiation by electrons in such a field has been studied by several groups[3,9,10] and also in more general studies.[4,12]

In the present article we make the decomposition into polarization components of wiggler radiation adopted by Sokolov and Ternov[18] for synchrotron radiation. This decomposition is more convenient from the point of view of experimental verification, since in this case the orientation of the components of the electric field strength vector of the radiation no longer depends on the direction of the radiation. This permits the entire radiated energy of an ultra-relativistic electron to be decomposed into two components: perpendicular to the magnetic field ($\sigma$) and directed along the field ($\pi$).

This approach has permitted us to advance substantially further than Refs. 9 and 10 in the analysis of the actually observed properties of wiggler radiation, particularly of the polarization, and to study the characteristics of the second harmonic of the radiation, which is well known[10,19] not to be emitted in the direction of the axis of the wiggler radiation cone and has been little studied. The detailed experimental study described below on the spectral and polarization properties of wiggler radiation as a function of angle for a wiggler installed in the ring of an electron synchrotron substantially fills in the gaps in the experimental information and confirms the conclusions of the theoretical studies which have been made.

## I. THEORY

### §1. General formulas

Expanding the exact solutions of the equations of motion of an electron in a magnetic field of the form $H_z = H_0 \sin(x/\lambda)$, $H_y = H_x = 0$ (Ref. 20) in a series in the small parameter $k = eH_0\lambda/m\gamma\beta c^2$, we obtain

$$x = V_0 t + {}^1/_8 k^2 \lambda \sin 2\omega_0 t, \quad y = k\lambda \cos \omega_0 t, \qquad (1)$$

where $\omega_0 = 2\pi V_0/\lambda_0$, $\lambda_0 = 2\pi\lambda$ is the spatial period of the magnetic field, $V_0 = \beta_0 c = V(1-k^2/4)$ is the longitudinal drift velocity of the particle, $V = \beta c$ is the total velocity of the particle, and $\gamma = (1-\beta^2)^{-1/2}$. It is more realistic to consider motion with initial conditions $t_0 = 0$, $y = \lambda$ for $t < t_0$, but in this case the formulas describing the radiation from the electron are very cumbersome and contain a series of incomple Anger-Weber functions.[21] We shall find the spectral-angular distribution of the electron's radiation in a system consisting of $N$ periods of the field with the initial conditions $t_0 = -\pi/2\omega_0$, $y = 0$ for $t < t_0$. We expand the Fourier component of the vector potential into the components:

$$\mathbf{A}(\omega) = \mathbf{e}_\alpha A_\sigma(\omega) + \mathbf{e}_\vartheta A_\pi(\omega),$$

$$\mathbf{e}_\alpha = (-\sin\alpha, \cos\alpha, 0), \quad \mathbf{e}_\vartheta = (\cos\vartheta\cos\alpha, \cos\vartheta\sin\alpha, -\sin\vartheta),$$

where $\mathbf{e}_\alpha$ and $\mathbf{e}_\vartheta$ are the unit vectors of the spherical coordinate system. Thus, integrating over time in $\mathbf{A}(\omega)$ (Ref. 22) and raising to the square, we find the spectral-angular distribution of the energy radiated by the electron:

$$\frac{dE_\pi}{d\Omega\,d\omega} = \frac{e^2 v^2 n_z}{c(1-\beta_0 n_z)^2(1-n_z^2)} \frac{\sin^2 \pi\nu N}{\sin^2 \pi\nu} \left[ L_\nu(p,q) - \frac{\sin\pi\nu}{\pi\nu} \right]^2, \qquad (2)$$

$$\frac{dE_\sigma}{d\Omega\,d\omega} = \frac{e^2 v^2}{c(1-\beta_0 n_z)^2(1-n_z^2)n_z^2} \frac{\sin^2 \pi\nu N}{\sin^2 \pi\nu} \left\{ \left[ L_\nu(p,q) - \frac{\sin\pi\nu}{\pi\nu} \right] n_y \right.$$
$$\left. - \frac{1}{2} k\beta_0(1-n_z^2)[L_{\nu-1}(p,q) - L_{\nu+1}(p,q)] \right\}^2, \qquad (3)$$

where

$$L_\nu(p, q) = \frac{1}{2\pi} \int_{-\pi}^{\pi} \exp[i(\nu\alpha - p\sin\alpha - q\sin 2\alpha)]d\alpha$$

$$= \sum_{k=-\infty}^{\infty} J_k(q) J_{\nu+2k}(p),$$

$$p = \frac{\omega}{\omega_0} k\beta_0 n_y, \quad q = -\frac{\omega}{8\omega_0} k^2\beta_0 n_x, \quad \nu = \frac{\omega}{\omega_0}(1-\beta_0 n_x),$$

$n_x$, $n_y$, and $n_z$ are the projections of the unit vector of the direction of radiation on the coordinate axes, and $J_\nu(x)$ is the Anger function. In deriving Eqs. (2) and (3) we used the recurrence relation

$$L_{\nu+2}(p, q) + L_{\nu-2}(p, q) = \frac{\nu}{q}\left\{L_\nu(p, q) - \frac{p}{2\nu}\right.$$

$$\times [L_{\nu+1}(p, q) + L_{\nu-1}(p, q)] - \left.\frac{\sin\pi\nu}{\pi\nu}\right\}.$$

Some properties of the function $L_\nu(p, q)$ for integral $\nu$ have been investigated in Ref. 23.

If in Eqs. (2) and (3) we divide by the time

$$\Delta t_p = (2\pi N/\omega_0)(1-\beta_0 n_x),$$

during which the entire radiated energy is received, and sum over the polarizations and let $N \to \infty$, we obtain the spectral-angular distribution of the intensity of radiation of an infinite wiggler.[9,10]

For an ultrarelativistic electron the distribution of the radiated energy in a finite system takes the following form:

$$\frac{dE_\pi}{d\omega d\Omega} = \frac{4e^2\nu^2\psi^2\sin^2\varphi}{c\varepsilon^2(1+\psi^2)^2} \frac{\sin^2\pi\nu N}{\sin^2\pi\nu}\left[L_\nu(p, q) - \frac{\sin\pi\nu}{\pi\nu}\right]^2, \quad (4)$$

$$\frac{dE_\sigma}{d\omega d\Omega} = \frac{4e^2\nu^2}{c\varepsilon^2(1+\psi^2)^2} \frac{\sin^2\pi\nu N}{\sin^2\pi\nu}\left\{\left[L_\nu(p, q) - \frac{\sin\pi\nu}{\pi\nu}\right]\psi\cos\varphi\right.$$

$$\left. - \frac{1}{(2+16\xi^2)^{1/2}}[L_{\nu+1}(p, q) + L_{\nu-1}(p, q)]\right\}^2, \quad (5)$$

where

$$\nu = \frac{\omega\varepsilon^2}{2\omega_0}(1+\psi^2), \quad \varepsilon^2 = \gamma^{-2}\left(1+\frac{1}{8\xi^2}\right), \quad (6)$$

$$p = \frac{4\nu_0\psi\cos\varphi}{\xi(16\xi^2+2)^{1/2}}, \quad q = -\frac{\nu_0}{2(1+8\xi^2)}. \quad (7)$$

Here $\psi = \theta/\varepsilon$ is the reduced angle of observation of the radiation, $\theta$ is the angle between the direction of observation and the $X$ axis, $\varphi$ is the azimuthal angle in the YOZ plane (measured from the $Y$ axis), and $\xi^{-1} = 2k\gamma$. Setting $\psi = 0$ in Eqs. (4) and (5) and using the property

$$L_\nu(0, q) = \cos(\pi\nu/2)J_{\nu/2}(-q), \quad (8)$$

we obtain the spectrum in the direction of the axis of the radiation cone:

$$\frac{dE}{d\omega d\Omega} = \frac{4e^2\gamma^2\nu^2\xi^2}{c(1+8\xi^2)^2} \frac{\sin^2\pi\nu N}{\cos^2(\pi\nu/2)}[J_{(\nu-1)/2}(-q) - J_{(\nu+1)/2}(-q)]^2. \quad (9)$$

The corresponding expression for an infinite wiggler was obtained by Alferov et al.[10] The factor $\sin^2\pi\nu N/\sin^2\pi\nu$ in Eqs. (4) and (5) determines the basic characteristic properties of the wiggler radiation, which do not depend on the form of the electron trajectory. The spectrum of the radiation in some direction $\psi, \varphi$ consists, as is well known, of individual peaks associated with integral values of $\nu$, and the half-width of the peaks is $\Delta\nu = 1/N$.

If only radiation with a fixed frequency $\omega_f$ is recorded, then each harmonic in the angular distribution has the form of a narrow ring. By varying the frequency $\omega_f$ or the electron energy we can change the size of these rings. In study of the spectral-angular distribution it is convenient to introduce the parameter

$$\nu_0 = \omega_f\varepsilon^2/2\omega_0, \quad (10)$$

which can be called the number of the harmonic observed along the axis of the radiation cone ($\theta = 0$). We shall consider two cases.

1. If the electron energy is fixed but various frequencies of radiation are observed, it is possible to use the reduced angle $\psi$. Then the angular size of the ring of the $n$-th harmonic can be written in the form

$$\psi_n = (n/\nu_0 - 1)^{1/2}, \quad n = 1, 2, 3, \ldots \quad (11)$$

and for the half-width of the $n$-th harmonic in the angular distribution we can take the angle between the maximum and the next minimum of the radiation

$$\Delta\psi_n = (n/\nu_0 - 1 + 1/N\nu_0)^{1/2} - (n/\nu_0 - 1)^{1/2}. \quad (12)$$

If $\nu_0 < 1$, all harmonics are present in the angular distribution. With increase of the frequency $\omega_f$ the rings of the harmonics are contracted toward the center. Here the width of each harmonic at first decrease and at

$$\psi_n = \left[\frac{nN}{1+nN}\right]^{1/2}, \quad \nu_0 = n\frac{1+nN}{1+2nN},$$

reaches a minimum and then increases to a value $\Delta\psi_n = (nN)^{-1/2}$, after which the harmonic leaves the region of detection.

2. If the frequency $\omega_f$ is constant, the dependence of the size and width of the rings on the energy is determined by the following expressions:

$$\theta_n = \varepsilon(n/\nu_0 - 1)^{1/2}, \quad \Delta\theta_n = \theta_n[(1+1/N(n-\nu_0))^{1/2} - 1]. \quad (13)$$

At high energy values ($\nu_0 \ll 1$) the size and width of the rings are constant, and as the energy is changed the distribution of intensity within the rings changes. With decrease of the electron energy to values of the order $\nu_0 \approx 1$ and further, the rings of the harmonics begin to be drawn into the center, and their width increases continuously. For $\nu_0 = n + 1/N$ a harmonic leaves the region of observation.

From Eqs. (4) and (5) we can see a characteristic feature of wiggler radiation—dependence of the spectral-angular distribution on energy consists only in a change of scale in the variables $\nu$ and $\psi$. Integrating Eqs. (4) and (5) over the solid angle $d\Omega = \varepsilon^{-2}d\varphi d\psi^2$, we obtain a function which depends only on the magnetic field strength ($\xi$) and the variable $n = \omega/2\omega_0\gamma^2$. The dependence of the integrated radiation spectrum on the energy of the particles thus consists only of a change of scale along the frequency axis.

## §2. Spectral and angular distributions of the radiation in the dipole approximation

If the change in the direction of motion of the electron during the obtained period is significantly less than the

characteristic angle of the radiation $(k \ll \gamma^{-1})$, then $p \ll 1, q \ll p$. In this case the function $L_\nu(p,q)$ can be expanded in series in the small quantities $p$ and $q$:

$$L_\nu(p,q) \approx \frac{\sin \pi\nu}{\pi\nu}\left(1 + \frac{p\nu}{1-\nu^2}\right).$$

As a result the spectral-angular distribution of the first harmonic takes the rather simple form:

$$\frac{dE_\pi(1)}{d\omega d\Omega} = \frac{4e^2k^2\gamma^4}{\pi^2c(1+\psi^2)^4}f(\nu)\,\psi^4\sin^2 2\varphi,$$

$$\frac{dE_\sigma(1)}{d\omega d\Omega} = \frac{4e^2k^2\gamma^4}{\pi^2c(1+\psi^2)^4}f(\nu)\,(1-\psi^2\cos 2\varphi)^2, \tag{14}$$

where

$$f(\nu) = \frac{\nu^4\sin^2 \pi\nu N}{(1-\nu^2)^2}, \quad \nu = \frac{\omega}{2\omega_0\gamma^2}(1+\psi^2), \quad \psi = \theta\gamma. \tag{15}$$

If the motion is determined by the initial conditions $t_0 = 0, y, = \lambda$ for $t < t_0$, then instead of Eq. (15) we have

$$f(\nu) = \nu^2\sin^2 \pi\nu N/(1-\nu^2)^2. \tag{16}$$

For sufficiently large $N$ Eqs. (15) and (16) are practically equivalent, since the entire radiation is concentrated in the vicinity of $\nu = 1$. Integrating Eq. (16), we find the angular distribution of the polarization components:

$$\frac{dE_\pi(1)}{d\Omega} = \frac{2e^2k^2\gamma^6\omega_0N}{c(1+\psi^2)^5}\,\psi^4\sin^2 2\varphi,$$

$$\frac{dE_\sigma(1)}{d\Omega} = \frac{2e^2k^2\gamma^6\omega_0N}{c(1+\psi^2)^5}\,(1-\psi^2\cos 2\varphi)^2. \tag{17}$$

The combined angular distribution has the form

$$\frac{dE(1)}{d\Omega} = \frac{2e^2k^2\gamma^6\omega_0N}{c(1+\psi^2)^5}\,[(1+\psi^2)^2-4\psi^2\cos^2\varphi]. \tag{18}$$

As has been noted elsewhere,[12] in the dipole approximation the angular distribution and the polarization of the first harmonic coincide with the corresponding properties of synchrotron radiation.[18,24] A numerical calculation of the angular distribution of the first harmonic of wiggler radiation is given in Ref. 13. Integrating Eqs. (17) and (18) over the angles, we find the total energy radiated in the first harmonic:

$$E_\pi(1) = {}^1/_8 E(1), \quad E_\sigma(1) = {}^7/_8 E(1),$$

$$E(1) = 2e^2k^2\gamma^4\omega_0\pi N/3c. \tag{19}$$

Equations (14)–(19) were obtained in the approximation $\xi^{-1} \ll 1$, but if in them we replace $\gamma^{-2} = 1-\beta^2$ by

$$\varepsilon^2 = 1-\beta_0^2 = \gamma^{-2}(1+\xi^{-2}/8),$$

then they are applicable also in the region $\xi^{-1} \lesssim 1$. In this case

$$\nu = \frac{\omega\varepsilon^2}{2\omega_0}(1+\psi^2), \quad \psi = \frac{\theta}{\varepsilon}. \tag{20}$$

## §3. Angular distribution of the second harmonic

Formulas for the angular distribution of the second harmonic in the dipole approximation can be obtained from Eqs. (4) and (5) by expanding $L_\nu(p,q)$ to terms of order $k^2$:

$$L_\nu(p,q) \approx \frac{\sin \pi\nu}{\pi\nu}\left[1 - \frac{1}{4}p^2 + \frac{x\nu}{1-\nu^2} - \frac{2y\nu}{4-\nu^2} - \frac{1}{4}\frac{x^2\nu^2}{4-\nu^2}\right].$$
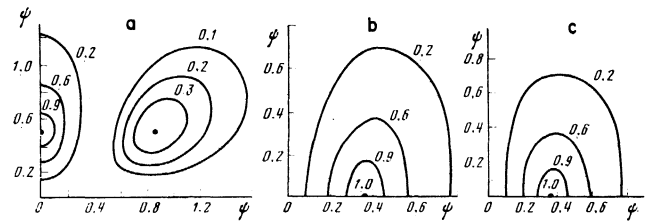


FIG. 1. Angular distribution of the second harmonic of wiggler radiation: a) the $\pi$ component, b) the $\sigma$ component, c) the combined angular distribution.

Integrating over frequency and neglecting terms of order $k^6$, we obtain the angular distribution of energy radiated by an electron in the second harmonic:

$$\frac{dE_\sigma(2)}{d\Omega} = \frac{2e^2k^4\gamma^8\omega_0N\psi^2\cos^2\varphi}{c(1+\psi^2)^7}(5+5\psi^2-8\psi^2\cos^2\varphi)^2,$$

$$\frac{dE_\pi(2)}{d\Omega} = \frac{2e^2k^4\gamma^8\omega_0N\psi^4\sin^2\varphi}{c(1+\psi^2)^7}(1+\psi^2-8\psi^2\cos^2\varphi)^2.$$

As an illustration we have shown in Fig. 1 by the contour lines of equal radiated energy the angular distribution of the second harmonic of wiggler radiation. Since the radiation is symmetric about the vertical and horizontal axes, it is sufficient to show one quadrant of the angular distribution of the wiggler radiation cone. As can be seen from Fig. 1a, the $\pi$ component of the radiation consists of six clearly expressed peaks–four of which are observed in the directions $\psi = 1$, $\varphi = \pm\pi/6$; the other two are located at angles $\psi = 0.5$, $\varphi = \pm\pi/2$ and are due to the longitudinal oscillations of the electron in the wiggler.

The $\sigma$ component of the radiation (Fig. 1b) has two main peaks symmetric relative to the vertical plane and directed at an angle $\psi \approx 0.366$. In addition, in the horizontal plane there are two subsidiary maxima in the direction $\psi = 1.77$ and with a level of radiation ~400 times less than the principal peaks. In Fig. 1 we have indicated in relative units the level of the radiated energy, normalized to the larger of the characteristic peaks.

If radiation with a fixed frequency $\omega_f$ is observed, then a narrow ring at the angle $\psi_n = (2n\omega_0/\varepsilon^2\omega_f - 1)^{1/2}$ is delineated in the angular distribution. In this ring peaks are observed in the plane $\varphi = 0$, $\pi$, and for $\psi > 5/19)^{1/2}$ four peaks appear in the direction $\varphi_1$. In the vertical plane and on a line $\varphi_2$ there is no radiation. Here

$$\cos^2\varphi_1 = 5(1+\psi^2)/24\psi^2, \quad \cos^2\varphi_2 = 5(1+\psi^2)/8\psi^2.$$

The angular distribution of the combined intensity (Fig. 1c) is hardly different from that of the $\sigma$ component. The maximum values of the $\sigma$ component and of the combined distribution coincide, and the intensity at the maximum of the $\pi$ component is 14.3 times smaller.

## II. EXPERIMENTAL STUDY OF WIGGLER RADIATION

Wiggler radiation was first observed in the millimeter and submillimeter regions.[27] It has been studied in more detail in the microwave region.[28,29] These experiments used as a source of radiation the electron beams of linear accelerators with energy 0.6–100 MeV.

The radiation from ultrarelativistic electrons in the x-ray region has been observed in a wiggler by means of the external beam of the Arus accelerator.[30] Spontaneous and stimulated radiation in the infrared region have been observed in a helical wiggler described by Elias *et al.*[31] The first studies in the optical region were carried out in wigglers installed in cyclic accelerators.[15-17]

However, in all of the studies mentioned above, no systematic and comprehensive studies of the properties of wiggler radiation have been made up to the present time. We report below the main results of an experimental study of the radiation obtained in a plane magnetic wiggler installed in a straight section of the electron orbit of the 1.5-GeV synchrotron Sirius.[25] The system of iron-free magnets of the wiggler consists of nine main sections and two correcting sections which provide periodic motion of the electrons with a period length $\lambda_0 = 14$ cm and a number of periods $N = 5$.

## §1. EXPERIMENTAL METHOD AND ARRANGEMENT

The fact that the shape of the spectrum and the spectral and angular distributions, Eqs. (4)–(7), are independent of the energy in the variables $\nu$ and $\psi$ permits measurements to be made by a simple method which is much more accurate than direct spectrographic measurements.

The technique of recording the integrated spectrum is as follows: the radiation is transmitted through a light filter with a definite frequency $\omega_f$ and the amount of energy $\Delta E$ transmitted by the filter is measured with increase of the electron energy, as a result of the change of scale in frequency, the spectrum broadens and thus extends through the detection frequency $\omega_f$. The broadening of the spectrum of the frequency scale leads to a relative decrease of the transmission band of the light filter by a factor $\gamma^2$. However, this effect is compensated by the fact that with increase of the electron energy the total radiated power increases in proportion to $\gamma^2$ [see Eq. (19)]. Thus, if we associate with each measured value $\Delta E$ the corresponding value $n = \omega_f/2\omega_0\gamma^2$, then the resulting dependence $\Delta E(n)$ coincides aside from a constant factor with the dependence of the spectral function $dE/d\omega$ on $(\omega/2\omega_0\gamma^2)$.

The spectral and angular distributions of the radiation were recorded by means of a scanning diaphragm located beyond the light filter and having a rather small cross section $\Delta s$. Here it is necessary to take into account that with increase of the electron energy the solid angle in which the main part of the radiation is concentrated decreases as $\gamma^{-2}$, which leads to an increase of the angular density of radiation and to a corresponding increase of the quantity of energy $\Delta E$ passing through the diaphragm. Consequently, in order to obtain from the experimental results the spectral and angular distribution $dE/d\omega d\Omega$ as a function of $n$ and $\psi$, it is necessary to divide the result of each measurement $\Delta E$ by the corresponding value of $\gamma^2$ and to associate with it the value $\psi = \theta/\varepsilon$.

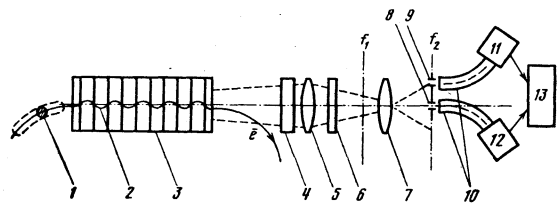The study of the spectral and angular distribution of



FIG. 2. Diagram of experiment.

wiggler radiation was carried out with the arrangement shown in Fig. 2. Radiation from an electron beam 1 moving along a trajectory 2 in a wiggler 3 is extracted from the vacuum through a window 4. An objective 5 with a focal length $f = 750$ mm forms an image of the angular distribution in the focal plane $f_1$. The objective 7 transfers the image $f_1$ with a magnification 6.5 to the plane $f_2$ where the measuring diaphragms 8 and 9 of dimeter 1 mm, corresponding to a solid angle $\Delta\Omega = 3.3\times10^{-8}$ sr, are located. Radiation which has passed through the diaphragms is transferred by the light pipes 10 to the photocathodes of the photomultipliers 11 and 12 whose output signals are fed to the input of the recording device 13. The wavelength of the radiation transversing the diaphragms 8 and 9 is determined by the interference light filter 5 with a wavelength at the maximum transmission $\lambda_f = 500$ nm and a bandwidth at half-height $\Delta\lambda_f = 10$ nm.

The variation of the photomultiplier output signal during the acceleration cycle is shown in Fig. 3 (curve 2). Against a background of monotonically rising synchrotron radiation we can see a peak due to the radiation of the electrons in the wiggler. The wiggler was turned on by means of the electron-energy monitoring circuit in such a way that at the moment of reaching a given energy the wiggler magnetic field strength was maximal. The moment of reaching the maximum of the magnetic field was determined by means of an induction probe placed in one of the central sections of the wiggler. The relative value of the electron energy was measured with an accuracy $\sim 10^{-4}$. Absolute values of the energy and the magnetic field strength were determined from the position of the maximum of the first harmonic in the radiation spectrum. Corresponding values of $\nu_0$ were calculated on the basis of Eq. (10). Determination of the signal corresponding to the wiggler radiation was carried out by the recording device 13 as follows: at the moments of time $t_1, t_2$, and $t_3$ the voltages $U_1$, $U_2$, and $U_3$ were recorded. Then from the total signal $U_2$ the synchrotron component was subtracted:

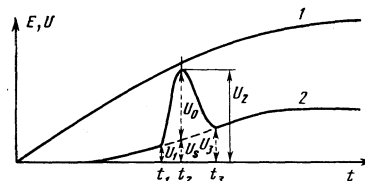$$U_s = U_1 + (U_3 - U_1)(t_2 - t_1)/(t_3 - t_1).$$



FIG. 3. Time dependence of electron energy (1) and photomultiplier output signal (2) in a single acceleration cycle.

Experiments were carried out in the electron energy range 70–800 MeV with variation of the magnetic field in the wiggler up to 3 kOe. With certain modes of wiggler operation and certain detection wave lengths we observed an excess of the spectral density of wiggler radiation over the synchrotron radiation by more than two orders of magnitude. The intensities of the wiggler and synchrotron radiation are proportional to the number of accelerated electrons, which changes from cycle to cycle. Therefore in the recording device 13 we provided a normalization of the wiggler radiation signal from diaphragm 8 to the synchrotron radiation signal from diaphragm 9 with averaging over 40 cycles. The synchrotron radiation was measured at the end of the acceleration cycle when its spectral density at the transmission wavelength of the light filter 6 does not depend on the energy of the particles. The experiment was carried out by remote control.

## §2. RADIATION SPECTRUM

In Fig. 4 the solid curve 1 shows the radiation spectrum in the direction of the wiggler axis, obtained with a magnetic field strength 398 Oe ($\xi^{-1} = 1.04$). The value of $n$ is plotted along the horizontal axis. The dashed line 1 is a curve plotted from Eq. (16) with inclusion of Eq. (20). The calculated spectrum has been normalized so that the areas under the solid and dashed curves coincide.

The observed broadening of the spectral line is due to the following causes: a) the finite bandwidth of the light filter: $\Delta n/n \approx 0.02$, b) the nonuniformity of the magnetic field in the region of beam traversal: $\Delta n/n \approx 0.012$, c) the spread in energy of the beam electrons $\Delta n/n \approx 10^{-3}$, and d) (the main contribution to broadening of the spectral line) the spread in the direction of motion of the beam electrons due to the betatron oscillations of the particles in the accelerator: $\Delta n/n \approx 0.036$. This same factor is responsible for the relative increase in the fraction of radiation in the low-frequency region.

With increase of the magnetic field strength the electron drift velocity decreases, which in accordance with the Doppler effect leads to a decrease of the frequency of radiation. The frequency at which the maximum of
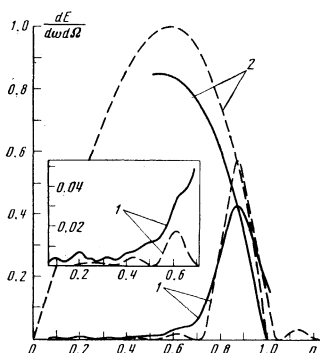


FIG. 4. Spectrum of wiggler radiation. The solid line is experimental and the dashed line is theoretical; 1—spectral distribution of first harmonic of wiggler radiation, 2—behavior of maximum of first harmonic for various magnetic field strengths.
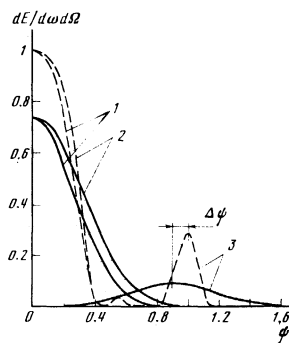


FIG. 5. Angular distribution of radiation. The solid line is experimental and the dashed line is theoretical. 1—in the horizontal plane; 2 and 3—in the vertical plane.

the first harmonic occurs is determined from the expressions (6): $n_{max} = (1 + 1/8\xi^2)^{-1}$. Simultaneously with the decrease of the frequency, the intensity of the radiation increases. As a result the maximum of the first harmonic shifts along the solid curve 2 (Fig. 4). For comparison we have shown by the dashed line 2 the line of the maxima plotted from the formula

$$\left(\frac{dE}{d\Omega d\omega}\right)_{max} = \frac{2e^2 N^2 \gamma^2}{c} (1-n)n[J_0(-q)-J_1(-q)]^2,$$

which was obtained from Eq. (9).

## §3. ANGULAR DISTRIBUTION

The angular distribution of wiggler radiation at wavelength $\lambda_f = 500$ nm obtained by means of the scanning diaphragm 8 is shown in Fig. 5. The magnetic field strength was 398 Oe ($\xi^{-1} = 1.04$). In accordance with the arrangement shown in Fig. 2, the angle $\theta$ is determined by the expression $\theta = r/fM$, where $r$ is the distance of the diaphragm from the axial direction, $f$ is the focal length of the objective 5, and $M$ is the magnification of the objective 7. The distributions 1 and 2 (Fig. 5) were obtained for an electron energy corresponding to the value $\gamma_1 = 398.6$. Curve 3 was obtained from a distribution measured at $\gamma_2 = \gamma_1\sqrt{2}$, multiplied by the ratio $(\gamma_1/\gamma_2)^2 = 1/2$ and with reduction to a universal angle $\psi$.

If a single electron radiated in the wiggler, the angular distribution reduced in this manner would be equivalent to the distribution of radiation of an electron with energy $\gamma$ at a wavelength $\lambda = 2\lambda_f$. However, the existence of an angular spread of the electrons in the beam leads to the result that with increasing energy of the particles the parameter $\eta = \sigma\gamma$ increases; this parameter determines the influence of the angular spread on characteristics of the radiation[32] ($\sigma$ is the dispersion of the electron angular spread). This explains this significant broadening of the distribution 3.

The dashed lines show the angular distribution constructed from Eqs. (14), (16), and (20) for $\nu_0 = 1$ (curves 1 and 2) and for $\nu_0 = 1/2$ (curve 3). The shift of the maximum $\Delta\psi$ in the experimental distribution 3 can be explained as follows. The light filter cuts out of the total angular distribution a narrow ring with an angular size given by Eq. (13). The radiation of the beam of electrons is made up of the rings produced by individual

electrons whose direction of radiation is determined by the angular spread. If we consider the distribution of the radiation in the vertical plane, the spread of the electrons in the vertical direction leads to a broadening of this distribution, and the horizontal spread produces in addition a displacement of the maximum toward the wiggler axis. From the broadening of the angular distributions it is possible to estimate the dispersion of the angular spread of the electrons in the beam, which in our case amounts to $\sigma \approx 6 \times 10^{-4}$ rad. Knowing the dispersion, we can estimate the rms amplitude of betatron oscillations in the accelerator.[32] For $\sigma = 6 \times 10^{-4}$ rad it is 6–7 mm, which coincides with the results obtained previously by other methods.[26]

## §4. Spectral and polarization distributions of wiggler radiation as a function of angle

To study the polarization and angular characteristics we recorded the wiggler radiation by means of an RFK-5 camera. Here the optical part of the apparatus with diaphragms 8 and 9 was used. In the plane $f_2$ we placed a photographic film, in front of which was mounted a Wollaston polarizing prism. The polarizing prism permitted simultaneous observation of the two mutually perpendicular polarization components, one of which was parallel to the plane of motion of the particles in the wiggler (the $\sigma$ component).

The current pulse exciting the wiggler consisted of a half-sine-wave of duration 0.7 msec, which was used as a natural gate in the recording process. During this time the relative change of the electron energy was ~0.01 and the shape of the angular distribution of the polarization components of the wiggler radiation was practically unchanged. The instability of the magnetic field strength did not exceed $5 \times 10^{-3}$. The relative increase of the width of the ring zones produced by the finite bandwidth of the light filter ($\Delta\lambda/\lambda \approx 0.02$) does not exceed 0.1.

A change of the magnetic field during the exposure should result in a strong smearing of the angular structure of the radiation. However, this process was significantly stabilized as a result of the fact that the radiated power is proportional to the square of the magnetic field strength, and at the level $H_{max}/\sqrt{2}$ ($H_{max} = 266$ Oe) the uncertainty in the angular coordinate was $\Delta\theta \approx 0.02$–0.1. In addition the choice of a high-contrast photographic material weakened significantly the blackening in the emulsion associated with small values of $H$.

With increase of the electron energy the width of the band not occupied by synchrotron radiation decreases, since radiation from the fringing fields of the straight section begins to move into the pass band of the filter. In order to decrease the integrated dose of synchrotron radiation in the region occupied by the wiggler radiation, the electron beam was dumped immediately on termination of the current pulse supplying the wiggler.

In Fig. 6 we have shown photographs of the angular distribution of the $\sigma$ and $\pi$ polarization components for various electron energies and a fixed wavelength $\lambda_f$ of
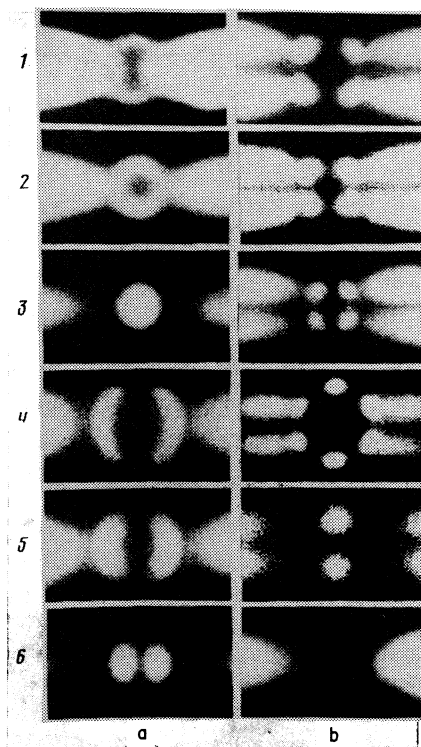


FIG. 6. Angular distribution of the $\sigma$ component (a) and of the $\pi$ component (b) of the polarization as a function of electron energy: $v_0$ is 0.566 (1a, 1b), 0.755 (2a, 2b), 1.13 (3a), 0.943 (3b), 1.51 (4a), 1.32 (4b), 1.70 (5a), 1.89 (5b), and 2.08 (6a).

wiggler radiation. Photograph 6b was made with the wiggler turned off.

With a high energy value the first harmonic occupies a ring zone of a large diameter (1). With decrease of the energy the diameter of the ring zone decrease (2, 3) and its width increases in accordance with Eq. (13). On further decrease of the energy the first harmonic leaves the filter pass band and the second harmonic becomes visible (4a–6a). The $\sigma$ component of the second harmonic has the form of two segments symmetric with respect to the vertical plane. With decrease of the energy the diameter of the ring zone of the segments decreases. A similar process of contraction of the ring zones is observed also in the $\pi$ component of the radiation (1b–5b). From the distribution of the intensity of radiation within the ring zones it is possible to deduce the shape of the total angular distribution of the $\sigma$ and $\pi$ polarization components.

As expected, the angular distribution of the first harmonic coincides with the instantaneous angular distribution of the synchrotron radiation.[12,18] This can be seen especially well in the case of the angular distribution of the $\pi$ component, which is characterized by the presence of four peaks symmetric relative to the axis of motion, while the $\sigma$ component has the form of an axially symmetric nucleus with a maximum in the direction of the axis of motion.

A characteristic feature of the distribution of the second harmonic is the presence of two intensity peaks in the $\sigma$ component and six peaks in the $\pi$ component of the radiation. For $v_0 = 1.32$ the ring zone of the second

harmonic has an angular size $\psi = 0.72$ and according to Fig. 1 encompasses all six peaks of the $\pi$ component. For $\nu_0 = 1.89$ (see Figs. 6, 5b) we have the angle $\psi = 0.25$. Here only two peaks of the $\pi$ component fall in the ring zone, these two peaks being due to the first harmonic of the longitudinal oscillations of the electron in the wiggler. The location of the ring zones in the angular distribution was determined on the basis of Eq. (11): here good agreement was observed between the shape of the experimental angular distribution (Fig. 6) and the theoretical calculation (Fig. 1), and also good agreement with Figs. 1 and 3 in Ref. 13.

## CONCLUSION

Our experimental study of wiggler radiation demonstrates good agreement with the conclusions of the theory. Such important properties of this radiation as the low angular divergence $(\sim \gamma^{-1})$, the high degree of polarization, the controlled and quasimonochromatic spectral composition of the radiation, and the possibility, no less important, of accurate calculation of the parameters of the radiation for any specific parameters of the electron beam and the periodic magnetic system, permit use of wiggler radiation for solution of a broad group of scientific and practical problems. The investigations have shown that by using a wiggler with a sufficiently large number of magnetic-field periods it is possible to determine the dispersion of the angular spread of the charged particles in the beam on the basis of the broadening of the spectral lines or the rings in the angular distribution of the wiggler radiation. The method developed for detection of the spectrum permits solution also of the inverse problem: from the location of at least two peaks of the first harmonic of the wiggler radiation on the $n$ scale (Fig. 4), to measure the absolute values of the electron energy and the magnetic field strength in the apparatus if the relative values $\varkappa = \gamma_2 / \gamma_1 = (n_{max}/n_{max})^{1/2}$ and $h = H_{02}/H_{01}$ are known:

$$\gamma_1 = \left( \frac{\lambda_0}{2\lambda_f} \frac{1-h^2}{\varkappa^2 - h^2} \right)^{1/2} ; \quad H_{01} = \frac{\pi m c^2}{e \lambda_0} \left( \frac{8(1-\varkappa^2)}{\varkappa^2 - h^2} \right)^{1/2} .$$

In the experiment the $n$ scale (Fig. 4), the values of $\nu_0$ (Fig. 6), the particle energies, and the magnetic field strengths were obtained with improved accuracy by this means.

[1] V. L. Ginzburg, Izv. AN SSSR, seriya fiz. 11, 165 (1947).

[2] H. Motz, J. Appl. Phys. 22, 527 (1951); H. Motz et al., 24, 826 (1953).

[3] N. A. Korkhmazyan, Izv. AN Arm. SSSR, Fizika 7, 114 (1972).

[4] V. N. Baĭer, V. M. Katkov, and V. M. Strakhovenko, Zh. Eksp. Teor. Fiz. 63, 2121 (1972) [Sov. Phys. JETP 36, 1120 (1973)].

[5] D. F. Alferov, Yu. A. Bashmakov, and E. G. Bessonov, Zh. Tekh. Fiz. 42, 1921 (1972) [Sov. Phys. Tech. Phys. 17, 1540 (1973)].

[6] M. M. Nikitin and A. F. Medvedev, Izv. vuzov, Fizika, No. 10, 135 (1974).

[7] L. M. Barkov, V. B. Baryshev, G. N. Kulipanov, N. A. Mezentsev, V. F. Pindyurin, A. N. Skrinskiĭ, and V. M. Khorev, Preprint IYaF 78-13, Nuclear Physics Institute, Novosibirsk, 1978.

[8] M. M. Nikitin and A. F. Medvedev, Izv. vuzov, Fizika, No. 8, 85 (1975).

[9] Yu. G. Pavlenko, V. I. Petukhov, and A. Kh. Mussa, Izv. vuzov, Fizika, No. 10, 88 (1973).

[10] D. F. Alferov, Yu. A. Bashmakov, and E. G. Bessonov, Trudy FIAN (Proceedings of the Lebedev Institute) 80, 100 (1975).

[11] V. G. Bagrov, V. R. Khalilov, A. A. Sokolov, and I. M. Ternov, Ann. Phys. (Leipzig) 30, 1 (1973).

[12] V. G. Bagrov, D. M. Gitman, A. A. Sokolov, I. M. Ternov, N. I. Fedosov, and V. R. Khalilov, Zh. Tekh. Fiz. 45, 1948 (1975) [Sov. Phys. Tech. Phys. 20, 1226 (1975)].

[13] M. M. Nikitin and V. Ya. Épp, Zh. Prikl. Spektrosk. 23, 1084 (1975) [J. Appl. Spectros. (USSR)].

[14] M. M. Nikitin and A. F. Medvedev, Zh. Tekh. Fiz. 45, 950 (1975) [Sov. Phys. Tech. Phys. 20, 600 (1975)].

[15] D. F. Alferov, Yu. A. Bashmakov, K. A. Belovintsev, E. G. Bessonov, and P. A. Cherenkov, Pis'ma Zh. Eksp. Teor. Fiz. 26, 525 (1977) [JETP Lett. 26, 385 (1977)].

[16] D. F. Alferov, Yu. A. Bashmakov, K. A. Belovintsev, E. G. Bessonov, A. M. Lifshits, V. V. Mikhaĭlin, and P. A. Cherenkov, Pis'ma Zh. Tekh. Fiz. 4, 625 (1978) [Sov. Tech. Phys. Lett. 4, 251 (1978)]

[17] A. N. Didenko, A. V. Kozhevnikov, A. F. Medvedev, and M. M. Nikitin, Pis'ma Zh. Tekh. Fiz. 4, 689 (1978) [Sov. Tech. Phys. Lett. 4, 277 (1978)].

[18] Sinkhrotronnoe izluchenie (Synchrotron Radiation), ed. by A. A. Sokolov and I. M. Ternov, Nauka, 1966.

[19] V. G. Bagrov, A. A. Sokolov, I. M. Ternov, N. I. Fedosov, and V. R. Khalilov, Izv. vuzov, Fizika, No. 1, 50 (1974).

[20] R. Combe and M. Feix, in: Millimetrovye i submillimetrovye volny (Millimeter and Submillimeter Waves), IIL, 1959, p. 240.

[21] E. Jahnke, F. Emde, and F. Lösch, Tables of Higher Functions, McGraw-Hill, 1960. Russian translation, Moscow, 1964, p. 288.

[22] J. D. Jackson, Classical Electrodynamics, Wiley, 1962, Russ. transl., Mir, 1965.

[23] A. I. Nikishov and V. I. Ritus, Zh. Eksp. Teor. Fiz. 46, 776 (1964) [Sov. Phys. JETP 19, 529 (1964)].

[24] V. G. Bagrov, V. A. Bordovitsyn, G. F. Kopytov, and V. Ya. Épp, Izv. vuzov, Fizika, No. 1, 46 (1974).

[25] A. A. Vorob'ev, I. P. Chuchalin, A. G. Vlasov, V. N. Kuz'min, G. A. Sipaĭlov, B. A. Solntsev, G. P. Fomenko, and P. M. Shchanin, Sinkhrotron TPI na 1.5 GeV (The 1.5-GeV Synchrotron at the Tomsk Polytechnic Institute), Atomizdat, 1968.

[26] A. V. Kozhevnikov, M. M. Nikitin, and A. F. Medvedev, Izv. vuzov, Fizika, No. 10, 115 (1971).

[27] H. Motz, W. Thon, and R. N. Whitehurst, J. Appl. Phys. 24, 826 (1953); Russ. transl. in "Millimetrovye i submillimetrovye volny," IIL, 1959, p. 317.

[28] M. Friedman and M. Herndon, Phys. Rev. Lett. 29, 55 (1975).

[29] Yu. V. Tkach, Ya. B. Faĭnberg, N. P. Gadetskiĭ, E. A. Lemberg, V. V. Dyatlova, V. V. Ermolenko, and A. V. Sidel'nikova, Pis'ma Zh. Eksp. Teor. Fiz. 22, 136 (1975) [JETP Lett. 22, 62 (1975)].

[30] A. I. Alikhanyan, S. K. Esin, K. A. Ispiryan, S. A. Kankanyan, N. A. Korkhmazyan, A. G. Oganesyan, and A. G. Tamanyan, Pis'ma Zh. Eksp. Teor. Fiz. 15, 142 (1972) [JETP Lett. 15, 98 (1972)].

[31] L. R. Elias, W. M. Fairbank, J. M. J. Madey, H. A. Schwettman, and T. I. Smith, Phys. Rev. Lett. 36, 717 (1976).

[32] M. M. Nikitin and V. Ya. Epp, Zh. Tekh. Fiz. 46, 2386 (1976) [Sov. Phys. Tech. Phys. 21, 1404 (1976)].

Translated by Clark S. Robinson